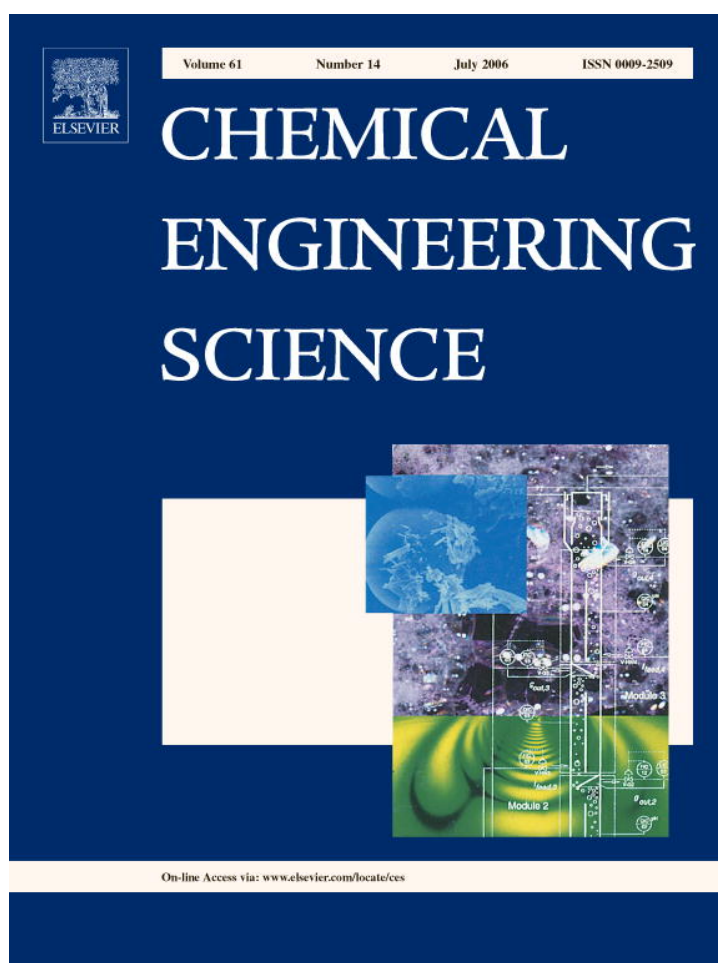


Provided for non-commercial research and educational use only.
Not for reproduction or distribution or commercial use.



This article was originally published in a journal published by Elsevier, and the attached copy is provided by Elsevier for the author's benefit and for the benefit of the author's institution, for non-commercial research and educational use including without limitation use in instruction at your institution, sending it to specific colleagues that you know, and providing a copy to your institution's administrator.

All other uses, reproduction and distribution, including without limitation commercial reprints, selling or licensing copies or access, or posting on open internet sites, your personal or institution's website or repository, are prohibited. For exceptions, permission may be sought for such use through Elsevier's permissions site at:

<http://www.elsevier.com/locate/permissionusematerial>

The simulation of microwave heating of wood using a rectangular wave guide: Influence of frequency and sample size

P. Rattanadecho

Faculty of Engineering, Thammasat University, Rangsit Campus, Pathumthani 12121, Thailand

Received 21 September 2005; received in revised form 27 February 2006; accepted 1 March 2006
Available online 7 March 2006

Abstract

Microwave heating–drying of wood using a wave guide is a relatively new area of research. In order to gain insight into the phenomena that occur within the wave guide together with the temperature distribution in the wood, a detailed knowledge of absorbed power distribution is necessary. In this paper, a two dimensional numerical model is developed to predicted the distribution of electromagnetic fields (TE₁₀-mode), power and temperatures distributions within wood located in rectangular wave guide. A three dimensional finite difference time domain (FDTD) scheme is used to determine electromagnetic fields and absorbed power by solving the transient Maxwell's equations, and finite difference method is used to obtain unsteady temperature profiles. Temperature dependence of wood dielectric properties is simulated through an iterative process. The simulations are performed illustrating the influence of irradiation times, working frequencies and sample size. The presented modeling is used to identify the fundamental parameters and provides guidance for microwave drying of wood.

© 2006 Elsevier Ltd. All rights reserved.

Keywords: Microwave heating; Rectangular wave guide; Numerical; Wood

1. Introduction

In the past decade, there are many successful examples of microwave application including; the heating and drying of foods, heating and drying of ceramics, heating and drying of woods and vulcanizations of rubber. A number of other analyses of the microwave heating process have appeared in the recent literature (Ayappa et al., 1991, 1992; Saltiel and Datta, 1997; Tada et al., 1998; Ratanadecho et al., 2001, 2002; Rattanadecho, 2004; Basak, 2003, 2004).

Although most of previous investigations considered simulations of microwave heating in solid sample, a little effort has been reported on study of microwave heating of wood in a rectangular wave guide particularly full comparison between mathematical simulations and experimental data.

Generally, the microwave power absorbed was assumed to decay exponentially into the sample following the Lambert's law. However, this assumption is valid for the large dimension

samples where the depth of sample is much larger than the penetration depth (all microwave energy, except the reflected wave from the upper surface of the sample, is dissipated within the sample). For the thin samples where the depth of sample is much smaller than the penetration depth, heat transfer rate by microwave is faster. The reason is that the reflection and transmission components at each interface will contribute to the resonance of standing wave configuration inside the sample whereas resonance is completely absent for greater length scales (Ayappa et al., 1991).

In perspective, Lambert's exponential decay law cannot predict resonance. Therefore, the spatial variations of the electromagnetic field within thin samples must be obtained by solution of the Maxwell's equations. The two-dimensional models of the interactions between electromagnetic field and dielectric materials have been used previously to study numerous heating processes of wood in a variety of microwave applicator configurations such as rectangular wave guide and cavities (Perre and Turner, 1997; Zhao and Turner, 2000). Readers may refer to Metaxas and Meridith (1983) and Mujumdar (1995) for an introduction to heat and mass transfer in microwave processing.

E-mail address: ratphadu@engr.tu.ac.th.

Due to the limited amount of theoretical and experimental work on microwave heating of hygroscopic porous media such as wood reported to date, the various effects are not fully understood and numbers of critical issues remain unresolved. These effects of the irradiation time, working frequencies and sample size on heating pattern have not been systematically studied. This work, the formulation of mathematical model for the microwave heating of wood inside a rectangular wave guide, in which the microwave of TE_{10} mode operating at the specified frequencies, is employed. The mathematical models are solved numerically and compared with experimental data. In the present analysis, the effects of the irradiation time, working frequencies and sample size on heating pattern are investigated in details.

The result presented here provides a basis for fundamental understanding of microwave drying of wood.

2. Experimental configuration

Fig. 1 shows the experimental apparatus for microwave heating system. It was developed for the heating tests to validate the model simulation. This system (Fig. 1(a)) consisted of a microwave supply system and a hot air system. In the microwave supply system a magnetron generated the monochromatic wave of TE_{10} mode operating at a frequency of 2.45 GHz, a wave-guide transmitted the wave to the heating cavity, a directional coupler with power meters measured power components. A circulator with an air cooling load was installed in the system to absorb the reflected wave, a three-stub tuner was used to adjust the matching impedance into the heating cavity. In experiments, the microwave was transmitted along the z -direction of the rectangular wave guide with inside dimensions of 11 cm \times 5.461 cm toward a water load that was situated at the end of the wave

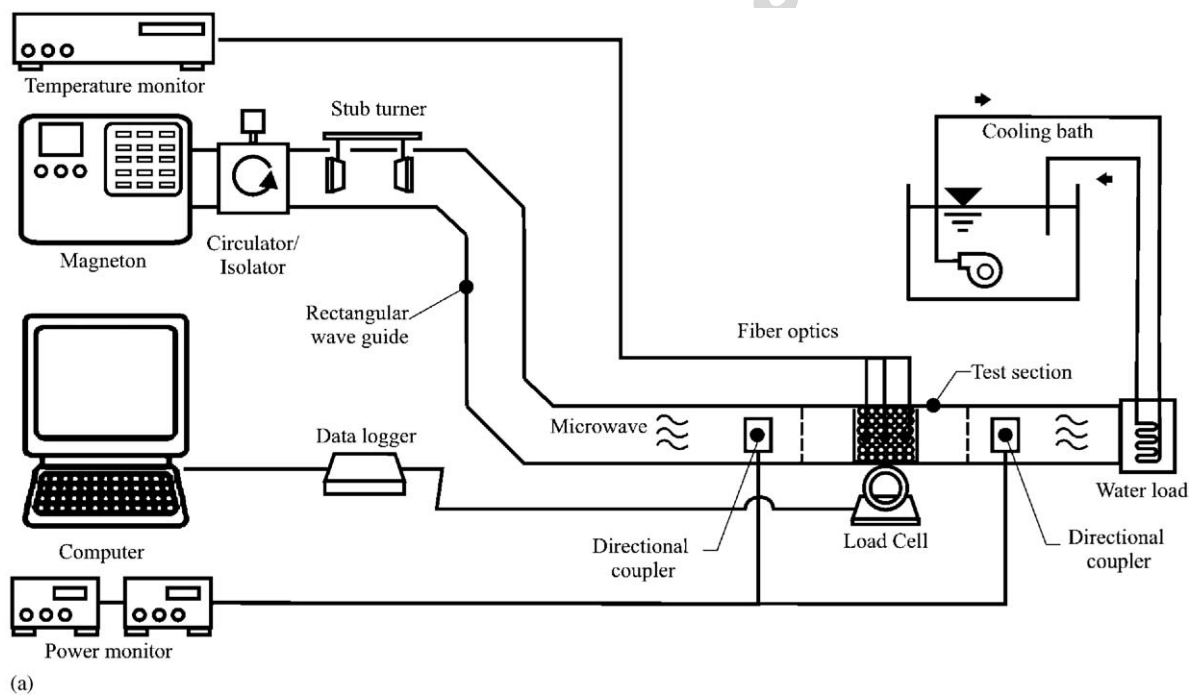


Fig. 1. Experimental apparatus: (a) microwave heating system; (b) wood sample.

Table 1
Dielectric properties of wood ($T = 25^\circ\text{C}$)

Frequency	2.45 GHz	5 GHz
Dielectric constant, ϵ'	1.591	1.591
Loss factor, ϵ''	0.033	0.033
Penetration depth (m)	0.0357	0.0175

guide. The water load ensured that only a minimal amount of microwave was reflected back to the sample. A cooling tower with an air cooled load was installed in the system to reduce the temperature in the water load system.

The wood sample with dimensions of $11\text{ cm} \times 5\text{ cm} \times 5.5\text{ cm}$ (Fig. 1(b)) filled in container is arranged in perpendicular to direction of irradiation via a rectangular wave guide. A sample container was made from polypropylene with a thickness of 0.075 cm, it did not absorb microwave energy.

During the experiment, output of magnetron was adjusted at the specified power (1000 W). The temperature distributions within the wood sample were measured using fiberoptic (LUXTRON Fluoroptic Thermometer, Model 790, accurate to $\pm 0.5^\circ\text{C}$). An infrared camera was used to detect the temperature distribution in the sample. All dielectric properties of wood are measured by using network analyzer which performs all of the necessary control functions, treatment of microwave signals, calculation, data processing and the results presentations. The dielectric properties of wood are listed in Table 1.

3. Analysis of microwave heating using a rectangular wave guide physical model

Fig. 2 shows the physical model of the microwave heating of wood using rectangular wave guide. Since the microwave field in the TE_{10} mode has no variation of field in the direction between the broad faces of rectangular wave guide, this means that the microwave is uniform in the y -direction. Consequently, it is assumed that two dimensional heat transfer model in the x and z directions would be sufficient to identify the microwave heating phenomena in a rectangular wave guide (Rattanadecho et al., 2001, 2002). The wood samples are assumed to be homogeneous and isotropic. Since the average moisture content of wood sample is low and the overall heating time is fast, the moisture loss is neglected. The other assumptions are as follows:

1. The absorption of microwave by air in rectangular wave guide is negligible.
2. The walls of rectangular wave guide are perfect conductors.
3. All materials are non-magnetic.
4. The effect of the sample container (made of poly propylene) on the electromagnetic and temperature fields can be neglected.

3.1. Maxwell's equation

Assuming the microwave is TE_{10} mode, the governing equations for the electromagnetic field can be written in term of the

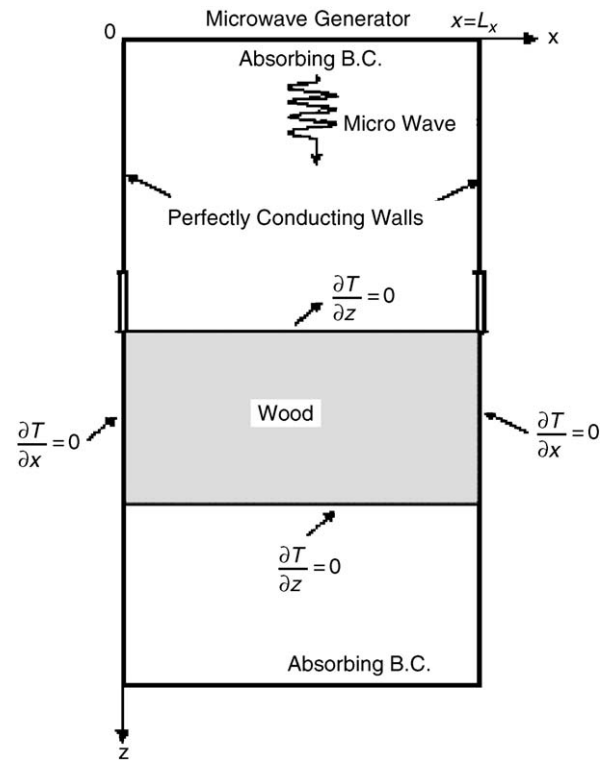


Fig. 2. Physical model.

component notations of electric and magnetic field intensities (Rattanadecho et al., 2002)

$$\frac{\partial E_y}{\partial z} = \mu \frac{\partial H_x}{\partial t}, \quad (1)$$

$$\frac{\partial E_y}{\partial x} = -\mu \frac{\partial H_z}{\partial t}, \quad (2)$$

$$-\left(\frac{\partial H_z}{\partial x} - \frac{\partial H_x}{\partial z}\right) = \sigma E_y + \epsilon \frac{\partial E_y}{\partial t}, \quad (3)$$

where E and H denote electric field intensity and magnetic field intensity, respectively. Subscripts x , y and z represent x , y and z components of vectors, respectively. Further, permittivity or dielectric constant ϵ , magnetic permeability μ and electric conductivity σ are given by

$$\epsilon = \epsilon_0 \epsilon_r, \quad \mu = \mu_0, \quad \sigma = 2\pi f \epsilon \tan \delta. \quad (4)$$

In addition, if magnetic effects are negligible, which is proven to be a valid assumption for most dielectric materials used in microwave heating applications, the magnetic permeability (μ) is well approximated by its value μ_0 in the free space.

Corresponding to the physical model shown in Fig. 2, boundary conditions are given as follows:

(a) Perfectly conducting boundaries; boundary conditions on the inner wall surface of a rectangular waveguide are given by using Faraday's law and Gauss' theorem:

$$E_t = 0, \quad H_n = 0. \quad (5)$$

The subscripts t and n denote the components of tangential and normal directions, respectively. (b) Continuity boundary condition; boundary conditions along the interface between different materials, for example between air and dielectric material surfaces, are given by using Ampere’s law and Gauss theorem:

$$E_t = E'_t, \quad H_t = H'_t, \quad D_n = D'_n, \quad B_n = B'_n. \quad (6)$$

The superscript $'$ denotes one of the different materials.

(c) Absorbing boundary condition; at both ends of the rectangular wave guide, the first order absorbing conditions are applied:

$$\frac{\partial E_y}{\partial t} = \pm v \frac{\partial E_y}{\partial z}. \quad (7)$$

Here, the symbol \pm represents forward or backward waves and v is phase velocity of the microwave.

(d) Oscillation of the electric and magnetic field intensities by magnetron; incident wave due to magnetron is given by the following equations:

$$E_y = E_{yin} \sin\left(\frac{\pi x}{L_x}\right) \sin(2\pi f t),$$

$$H_x = \frac{E_{yin}}{Z_H} \sin\left(\frac{\pi x}{L_x}\right) \sin(2\pi f t), \quad (8)$$

where E_{yin} is the input value of electric field intensity, L_x is the length of rectangular wave guide in x -direction. Z_H is the wave impedance defined as

$$Z_H = \frac{\lambda_g Z_I}{\lambda_0} = \frac{\lambda_g}{\lambda_0} \sqrt{\frac{\mu_0}{\epsilon_0}}. \quad (9)$$

3.2. Heat transport equation

The temperature of wood exposed to incident wave is obtained by solving the heat conduction equation with the microwave power absorbed included as a local electromagnetic heat generation term:

$$\frac{\partial T}{\partial t} = a \left(\frac{\partial^2 T}{\partial x^2} + \frac{\partial^2 T}{\partial z^2} \right) + \frac{Q}{\rho \cdot C_p}, \quad (10)$$

where, T is temperature, a is thermal diffusivity, ρ is density and c_p is heat capacity at constant pressure. The local electromagnetic heat generation term Q is directly depended upon the electric field distribution defined as:

$$Q = 2\pi \cdot f \cdot \epsilon_0 \cdot \epsilon_r (\tan \delta) E_y^2. \quad (11)$$

The initial condition of wood sample defined as: $T = T_0$ at $t = 0$. The boundary conditions for solving heat transport equation are shown in Fig. 2.

4. Numerical technique

In order to predict the electromagnetic field, a finite difference time domain (FDTD) method is applied. In this study, the leapfrog scheme is applied to the set of Maxwell’s

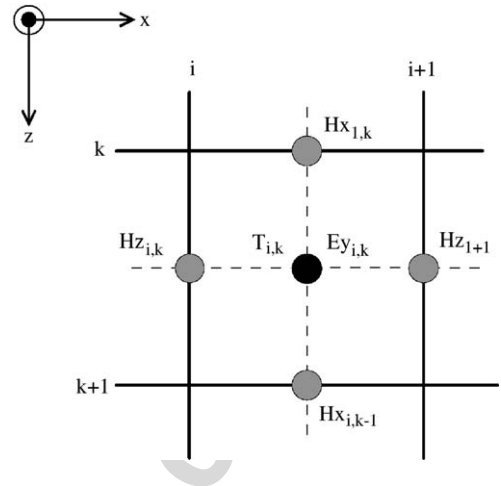


Fig. 3. Grid system configuration.

equations. The electric field vector components are offset one half cell in the direction of their corresponding components, while the magnetic field vector components are offset one half cell in each direction orthogonal to their corresponding components. The electric field and magnetic field are evaluated at alternative half time steps. For TE mode, the electric and magnetic field components are expressed by the total field FDTD equations as

$$E_y^n(i, k) = \frac{1 - (\sigma(i, k)\Delta t)/(2\epsilon(i, k))}{1 + (\sigma(i, k)\Delta t)/(2\epsilon(i, k))} E_y^{n-1}(i, k) + \frac{1}{1 + (\sigma(i, k)\Delta t)/(2\epsilon(i, k))} \frac{\Delta t}{\epsilon(i, k)} \times \left\{ \frac{-(H_z^{n-1/2}(i + 1/2, k) - H_z^{n-1/2}(i - 1/2, k))}{\Delta x} + \frac{(H_x^{n-1/2}(i, k + 1/2) - H_x^{n-1/2}(i, k - 1/2))}{\Delta z} \right\}, \quad (12)$$

$$H_x^{n+1/2}(i, k + 1/2) = H_x^{n-1/2}(i, k + 1/2) + \frac{\Delta t}{\mu(i, k + 1/2)} \times \left\{ \frac{E_y^n(i, k + 1) - E_y^n(i, k)}{\Delta z} \right\}, \quad (13)$$

$$H_z^{n+1/2}(i + 1/2, k) = H_z^{n-1/2}(i + 1/2, k) - \frac{\Delta t}{\mu(i + 1/2, k)} \times \left\{ \frac{E_y^n(i + 1, k) - E_y^n(i, k)}{\Delta x} \right\}. \quad (14)$$

Furthermore, the heat transport equation (Eq. (10)) is solved by the method of finite differences. The spatial and the temporal terms are approximated spatially using finite difference equations for electromagnetic field and temperature field, as shown in Fig. 3. Eqs. (12)–(14) and discretized heat transport equation

are solved on this grid system. The choice of spatial and temporal resolution is motivated by reasons of stability and accuracy.

To insure stability of the time-stepping algorithm, Δt must be chosen to satisfy the Courant stability condition:

$$\Delta t \leq \frac{\sqrt{(\Delta x)^2 + (\Delta z)^2}}{v} \quad (15)$$

and the spatial resolution of each cell is defined as:

$$\Delta x, \Delta z \leq \frac{\lambda_g}{10\sqrt{\epsilon_r}}. \quad (16)$$

Corresponding to Eqs. (15) and (16), the calculation conditions are as follows [4]:

- (1) To ensure that each wavelength of the microwave in the computational domain for each frequency has more than 10 subdivisions in the numerical calculation, thus, the computational domain is conservatively set such that the spatial resolution of each cell is $\Delta x = \Delta z \leq \lambda_{mg}/10\sqrt{\epsilon_r} \approx 1.0$ mm.
- (2) It should be noted that the time step length for the heat transfer Δt is of the order of one second, which is very large compared with the time step required for the FDTD scheme, which is of order of several picoseconds (Rattanadecho et al., 2002). Consequently, the different time steps of $\Delta t = 1$ [s] and $\Delta t = 1$ [ps] are used for the computation of temperature field and the electromagnetic field, respectively.
- (3) Relative errors in the iteration procedure of 10^{-8} were chosen.

5. The iterative computational schemes

Since the dielectric properties of wood are temperature dependent, to understand the influence of electromagnetic field on microwave heating realistically, it is necessary to consider the coupling between electric field and temperature field. For this reason, the iterative computational schemes are required to resolve the coupled non-linear Maxwell's equations and heat transport equations.

The computational scheme is to compute a local heat generation term by running an electromagnetic calculation with uniform properties, determined from initial temperature data. The electromagnetic calculation is performed until a sufficient period is reached in which a representative average rms (root-mean-square) of the electric field at each spatial point is obtained, typically 30 000 time steps. The microwave power absorption at each point is computed and used to solve the time dependent temperature field. Using these temperatures new values of the dielectric properties are calculated and used to re-calculate the electromagnetic fields and then microwave power absorption. The all steps are repeated until the required heating time is reached. The details of computational schemes and strategy are illustrated in Fig. 4.

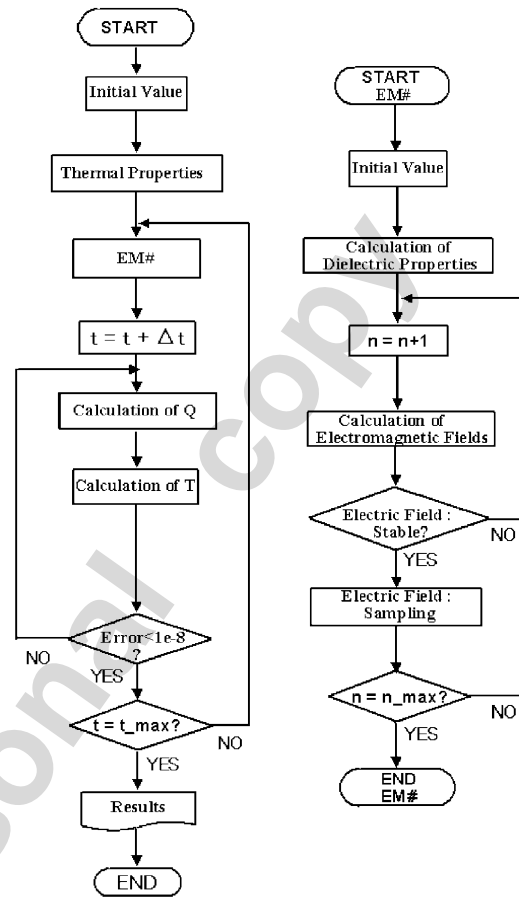


Fig. 4. Computational schemes.

6. Results and discussion

The experimental results for the microwave heating of wood were compared with predictions from mathematical model. The wood sample with a dry basis density of 721 kg/m^3 , moisture content of 12.5% and initial temperature of 25°C are used for the present analysis. Since the average moisture content of wood sample is very low and the overall heating time is fast, the moisture content was treated to be constant throughout the numerical calculation of microwave heating process. In the microwave industries, only a few frequencies are available. Currently, two frequencies, 2.45 and 5 GHz are utilized for testing the model.

The dielectric properties of wood were directly taken from present experiment. Some numerical values for dielectric constant and loss factor are listed in Table 1. The penetration depth D_p of wood at 25°C is approximately $D_p = 0.0357$ m (frequency of 2.45 GHz) and $D_p = 0.0175$ m (frequency of 5 GHz) according to the theoretical value

$$D_p = \frac{1}{2\pi f/v\sqrt{\frac{\epsilon_r'\sqrt{1+(\epsilon_r''/\epsilon_r')^2}-1}{2}}} = \frac{1}{2\pi f/v\sqrt{\frac{\epsilon_r'\sqrt{1+(\tan\delta)^2}-1}{2}}}, \quad (17)$$

the penetration depth values are listed in Table 1.

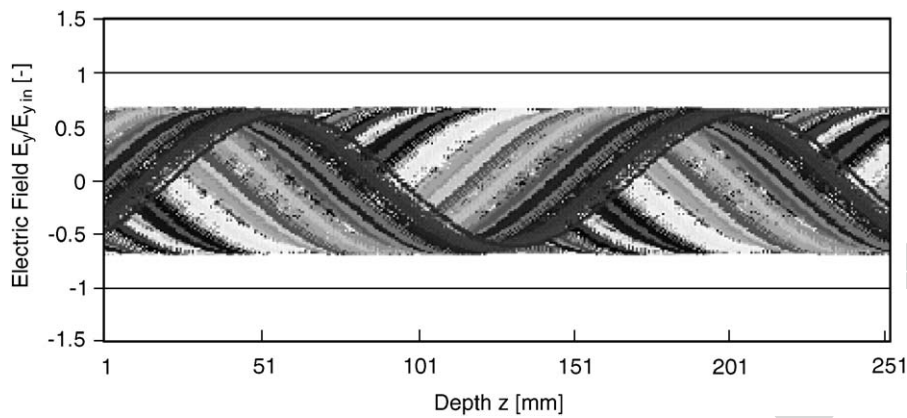


Fig. 5. The electric field distribution (Case 1).

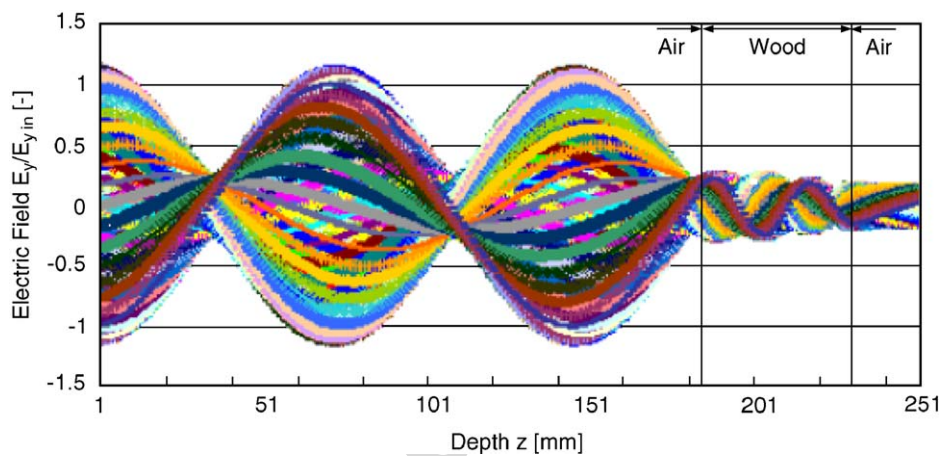


Fig. 6. The electric field distribution (Case 2).

From the definition of the penetration depth D_p the electric field intensity is the dielectric falls to approximately $1/e$ of its strength with distance D_p from the dielectric surface.

In this study, the effects of microwave frequencies and sample sizes on heating process are discussed in details.

6.1. The electric field distribution

To understand the electrical field distribution inside the rectangular wave guide and wood sample during microwave heating, the simulation analysis is required. The simulations of the typical electric field of TE_{10} mode along the center axis ($x=55$) of rectangular wave guide for specified heating conditions; $P = 1000$ W, $t = 30$ s and size = 11 cm (x : width) \times 5 cm (z : depth) are presented as follows:

- (1) Rectangular wave guide is empty, its dielectric constant is unity (which corresponds to that of air).
- (2) Rectangular wave guide is filled with wood sample, operating at the microwave frequency of 2.45 GHz (30 s).
- (3) Rectangular wave guide is filled with wood sample, operating at the microwave frequency of 5 GHz (30 s).

Fig. 5 shows the stationary wave inside the rectangular wave guide with completely absorbed power at the end of the wave guide (Case 1). It is observed that the electric field distribution displays a wavy behavior with an almost uniform amplitude along a rectangular wave guide without the sample. Fig. 6 shows the electric field distribution inside a rectangular wave guide during microwave heating with the frequency of 2.45 GHz (Case 2). Since the typical depth of wood is close to the penetration depth of microwave (see Table 1), thus a large part of microwaves are able to penetrate through the sample. The reflected wave will occur on each interface, from air (cavity) to upper surface and from lower surface of sample to air (cavity). The reflection and transmission components at each interface will contribute to the resonance of standing wave configuration inside the sample and give rise to a microwave absorption peak further from the surface exposed to incident microwaves. Furthermore, focusing attention of electric field pattern inside the cavity (left hand side), a stronger standing wave with a large amplitude is formed by interference between the incident and reflected wave from the surface of sample due to the difference of dielectric properties of materials (air and sample) at this interface. Owing to energy absorption, it is

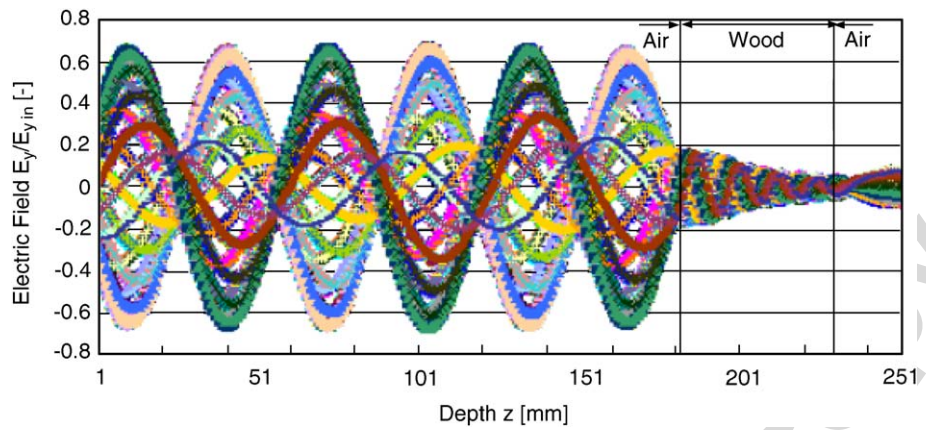
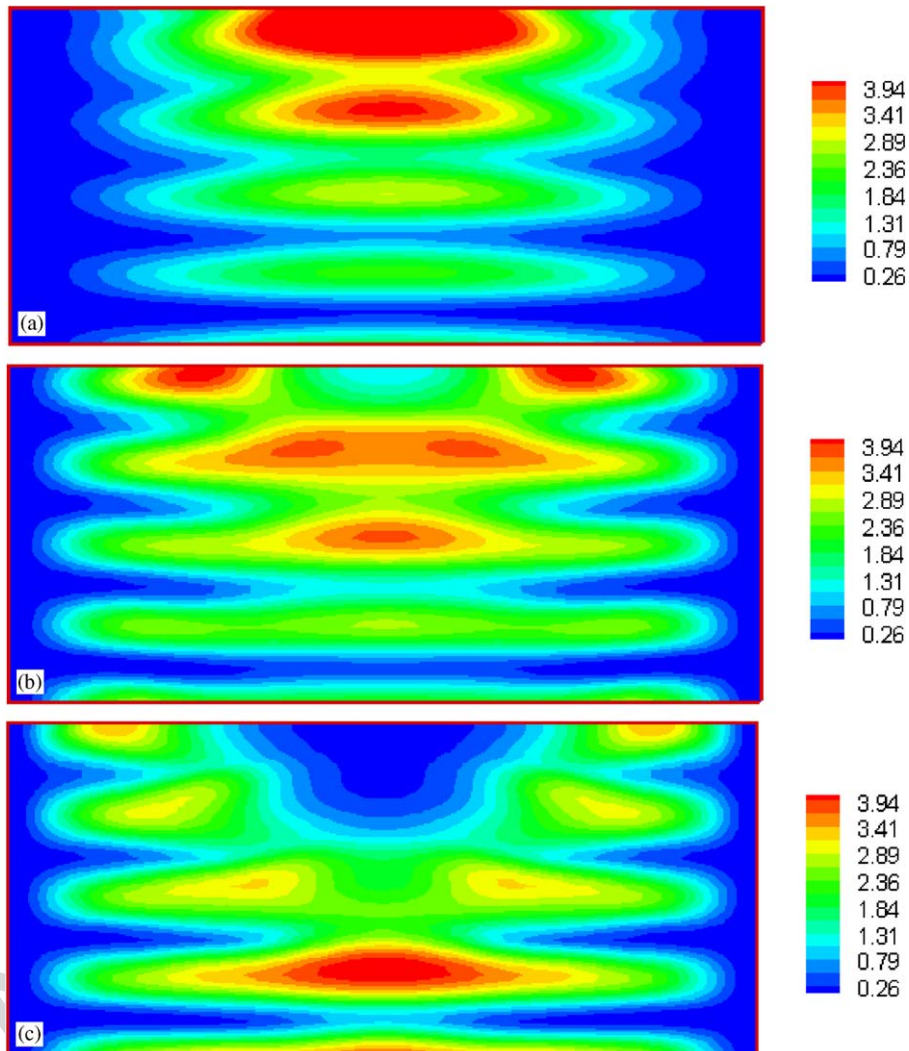


Fig. 7. The electric field distribution (Case 3).

Fig. 8. Microwave power absorbed (MW/m^3) at various heating times: (a) 10 s; (b) 20 s; (c) 30 s ($f = 2.45$ GHz, size = 11 cm (x) \times 5 cm (z)).

evident from the results that the electric field within the sample attenuates, and thereafter the absorbed energy is converted to the thermal energy, which increases the sample temperature.

Fig. 7 shows the electric field distribution when a sample of wood is inserted in the rectangular wave guide during microwave heating with a frequency of 5 GHz (Case 3). In contrast

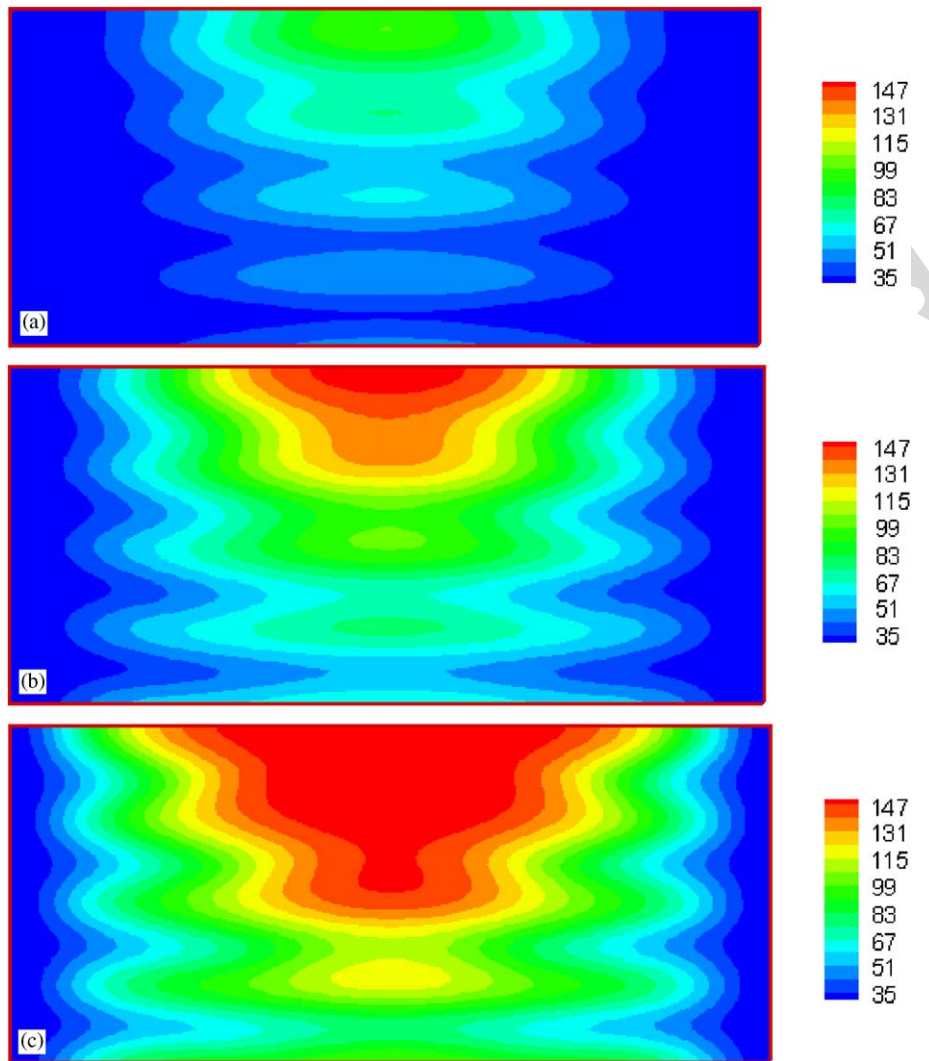


Fig. 9. Temperature distribution ($^{\circ}\text{C}$) at various heating times: (a) 10 s; (b) 20 s; (c) 30 s ($f = 2.45$ GHz, size = 11 cm (x) \times 5 cm (z)).

to the electric field configuration in case 2, which is a result of a transmitted wave at the incident face and a reflected wave from the lower surface of the sample. This is due to the fact that microwave operates at a high frequency has a short wavelength which corresponds to a smaller penetration depth of microwave (see Table 1) when compared with the depth of sample. Consequently, all microwaves, except the reflected wave from the upper surface of the sample, is absorbed by the sample. It is found that the wave amplitude diminishes after $z = 2$ cm, which results in a low microwave power absorbed. This phenomenon explains why the electric field and therefore the microwave power absorbed are the greatest at the surface exposed to incident microwaves and decay exponentially along the propagating direction with a very small wavelength.

6.2. Effect of frequency on temperature distribution

The predictions of temperature distribution for microwave heating of wood are shown in Figs. 8 and 9, which corresponds

to the initial temperature of 25°C and microwave power level of 1000 W. Here, microwaves are transmitted along the z -direction of the rectangular wave guide toward the top surface of a wood sample with a dimension of 11 cm (x : width) \times 5 cm (z : depth) in the xz -plane. Most importantly, the effects of the variation of frequency on temperature distribution are discussed by considering the two microwave frequencies ($f = 2.45$ GHz and 5 GHz).

For microwave heating of wood with the microwave frequency of 2.45 GHz, the temperature profile within the sample (Fig. 9) displays a wavy behavior corresponding to the resonance of electric field (Fig. 6). This is because the electric field within the sample attenuates owing to energy absorption, and thereafter the absorbed energy is converted to the thermal energy, which increases the sample temperature. It is found that the temperatures decay slowly along the propagation direction following the absorption of microwave (Fig. 8). The temperature distributions are shown for $t = 10, 20$ and 30 s, respectively. The maximum temperature within the sample is around 147°C at $t = 30$ s.

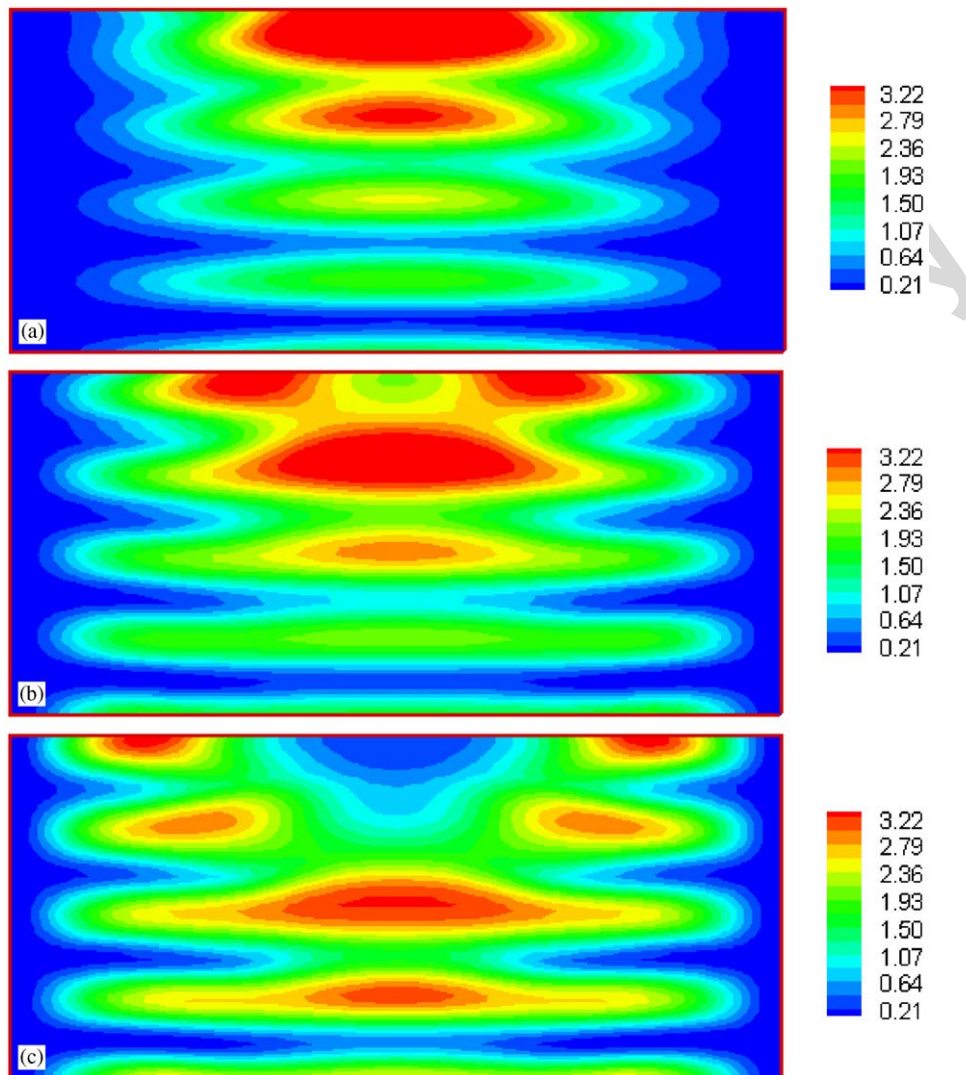


Fig. 10. Microwave power absorbed (MW/m^3) at various heating times: (a) 10 s; (b) 20 s; (c) 30 s ($f = 5 \text{ GHz}$, size = 11 cm (x) \times 5 cm (z)).

For microwave heating of wood with the microwave frequency of 5 GHz, the predictions of microwave power absorbed and temperature distributions are shown in Figs. 10 and 11, respectively. Since the higher microwave frequency leads to a much smaller penetration depth, and the electric field decays much faster as compared to that in the case of microwave frequency of 2.45 GHz. In contrast to that case of microwave frequency of 2.45 GHz, which results in a transmitted wave at the incident face and a reflected wave from the lower surface of the sample. In this case, the microwave that operates at a high frequency has a short wavelength which corresponds to a smaller penetration depth of microwave (see Table 1) compared with the depth of sample. Consequently, all microwaves, except the reflected wave from the upper surface of the sample, is absorbed by the sample. It is found that the wave amplitude diminishes after $z = 2 \text{ cm}$, which results in a low microwave power absorbed. This phenomenon explains why the electric field (Fig. 7) and therefore the microwave power absorbed are the greatest at the surface exposed to the incident microwaves,

and decay exponentially along the propagating direction with a very small wavelength, resulting in a thinner thermally stratified layer (Fig. 11). It is observed that the wavy behavior of the temperature distribution within the sample disappears and it is totally different from the previous case (as referred to Fig. 9). This is because the penetration depth of microwave drops dramatically and the wavelength is very small for this case. Since the reflected wave from the lower surface of the sample is almost negligible, no standing wave or resonance is formed within the sample (Fig. 7). Therefore, the microwave power absorbed decreases sharply to small value along the propagating direction ($z > 2 \text{ cm}$). Similar to the microwave power absorbed (Fig. 10), the temperature distribution significantly varies from the maximum temperature to the minimum temperature in a short distance and decays quickly. It is evident from the Fig. 11 that, in this case, there is only one peak appearing on the temperature distribution. The temperature distributions are shown for $t = 10, 20$ and 30 s , respectively. The maximum temperature within the sample is around 145°C at $t = 30 \text{ s}$.

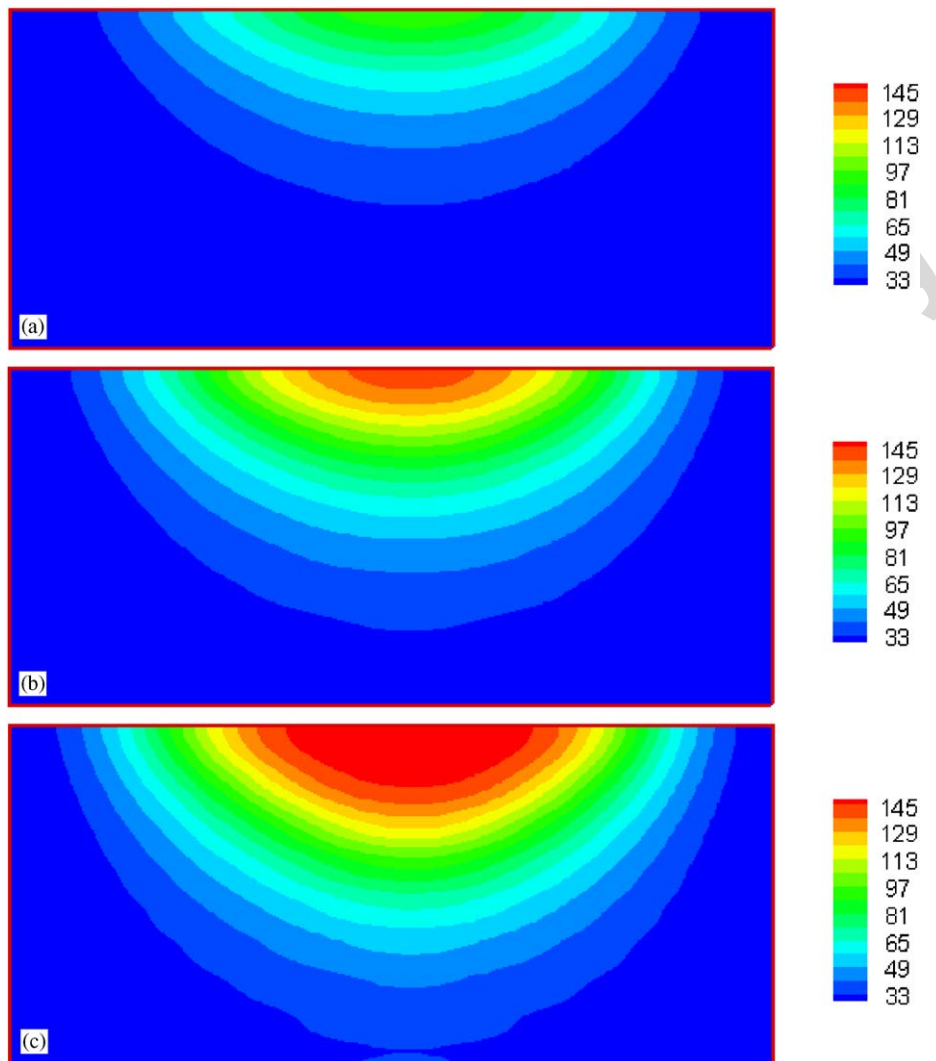


Fig. 11. Temperature distribution ($^{\circ}\text{C}$) at various heating times: (a) 10 s; (b) 20 s; (c) 30 s ($f = 5$ GHz, size = 11 cm (x) \times 5 cm (z)).

Considering the region along the propagation direction, the temperature distribution drops dramatically, and after $z > 2$ cm, the temperature distribution is almost unchanged within the heating time of 10 s.

6.3. Effect of sample size on temperature distribution

The predictions of temperature distribution for microwave heating of wood are discussed, which corresponds to the initial temperature of 25°C and microwave power level of 1000 W. The effects of the variation of sample sizes on temperature distribution are discussed by considering the two sample sizes (thin sample; size = 11 cm (width) \times 5 cm (depth) and thicker sample; size = 11 cm (width) \times 8 cm (depth)).

In Fig. 13, which corresponds to the microwave heating of thicker sample (size = 11 cm (width) \times 8 cm (depth)) in the xz -plane, it can be seen that the temperature distributions along the propagating wave does not show a clear evidence of wavy

behavior, which is inconsistent with what was exhibited in Fig. 9 for the thin sample. This figure highlights that the thicker sample has a different heating characteristics compared with the thin sample. This is because the standing wave or resonance has a substantial effect on the shape of the transient microwave power absorbed.

Furthermore, the maximum power absorbed (Fig. 12) and maximum temperature (Fig. 13) are lower for this case compared with those shown in Figs. 8 and 9. The temperature distributions are shown for $t = 10, 20$ and 30 s. The maximum temperature within the sample is around 146°C at $t = 30$ s.

Fig. 14 shows the predicted and experimental results of temperature distribution within the wood sample along with the horizontal axis of rectangular wave guide ($z = 0.5$ cm), which corresponds to the initial temperature of 25°C , microwave power level of 1000 W and frequency of 2.45 GHz. The result shows the greatest temperature displays in the center of wood sample with the temperature decreasing towards the side walls

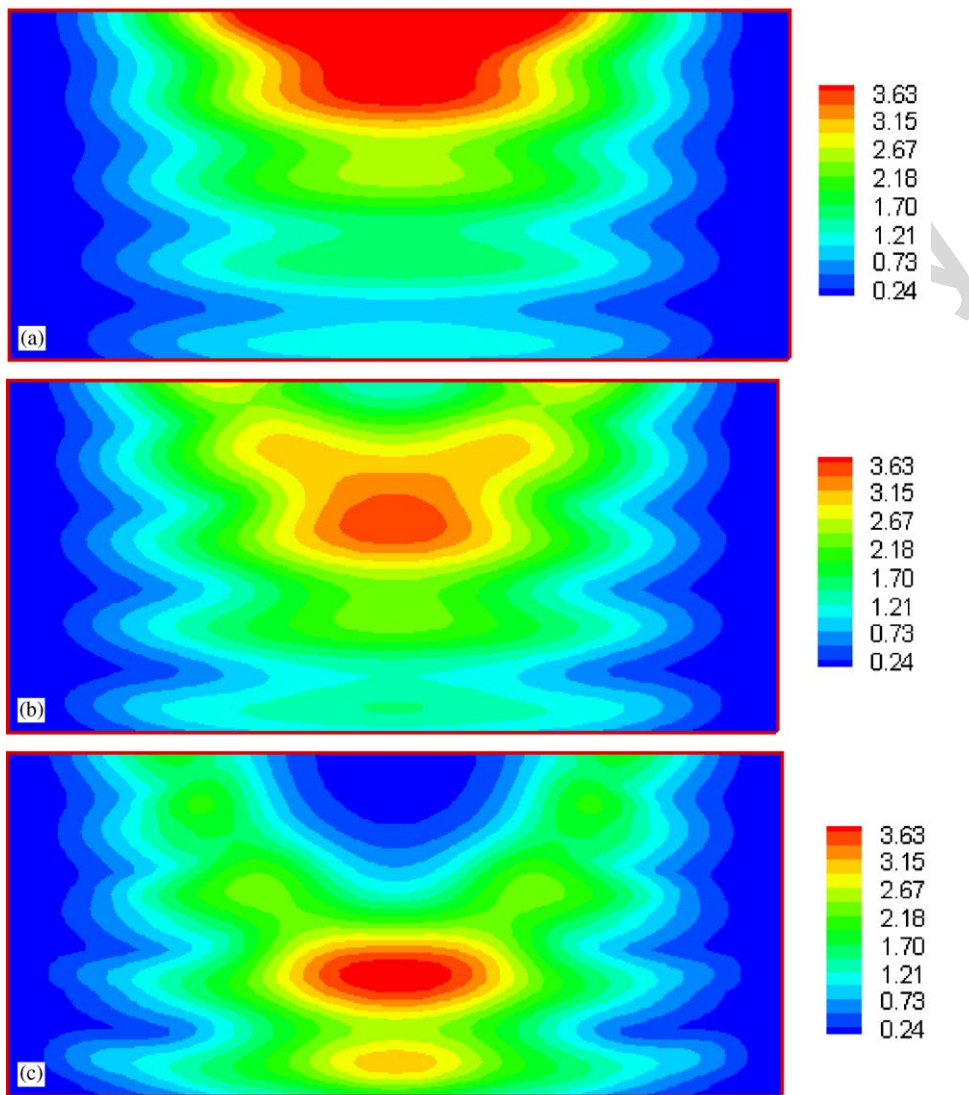


Fig. 12. Microwave power absorbed (MW/m^3) at various heating times: (a) 10 s; (b) 20 s; (c) 30 s ($f = 2.45$ GHz, size = 11 cm (x) \times 8 cm (z)).

of sample. This phenomenon occurs because the TE_{10} field pattern displays a maximum E -field at the center of wave guide. It is shown that the predicted results agree well with the experimental result for the microwave heating of wood. The prediction of temperature from the mathematical model is also compared with the experimental data measured by infrared camera for microwave heating of wood as shown in Fig. 15 ($t = 30$ s). It can be seen that the agreement between two heating patterns is qualitatively consistent, particularly in the hot spot region.

Therefore, the capability of the mathematical model to correctly handle the field variations is shown. With further quantitative validation of the mathematical model, it is clear that the model can be used as a real tool for the detail investigation in this particular microwave heating of wood samples at a fundamental level.

7. Conclusion

The numerical analysis presented in this paper describes many important interactions within wood samples during microwave heating using a rectangular wave guide. The following paragraph summarizes the conclusions of this study:

(1) A generalized mathematical model for microwave heating of wood is proposed. It is used successfully to describe the heating phenomena under various conditions.

(2) The influence of irradiation times, working frequencies and sample size on the microwave power absorbed and heating pattern that develop within wood samples is clarified in details. The simulated results for the temperature distribution within the wood samples rate are in agreement with experimental results. The main finding of the simulations are summarized again in Table 2. At a microwave frequency of 2.45 GHz the power

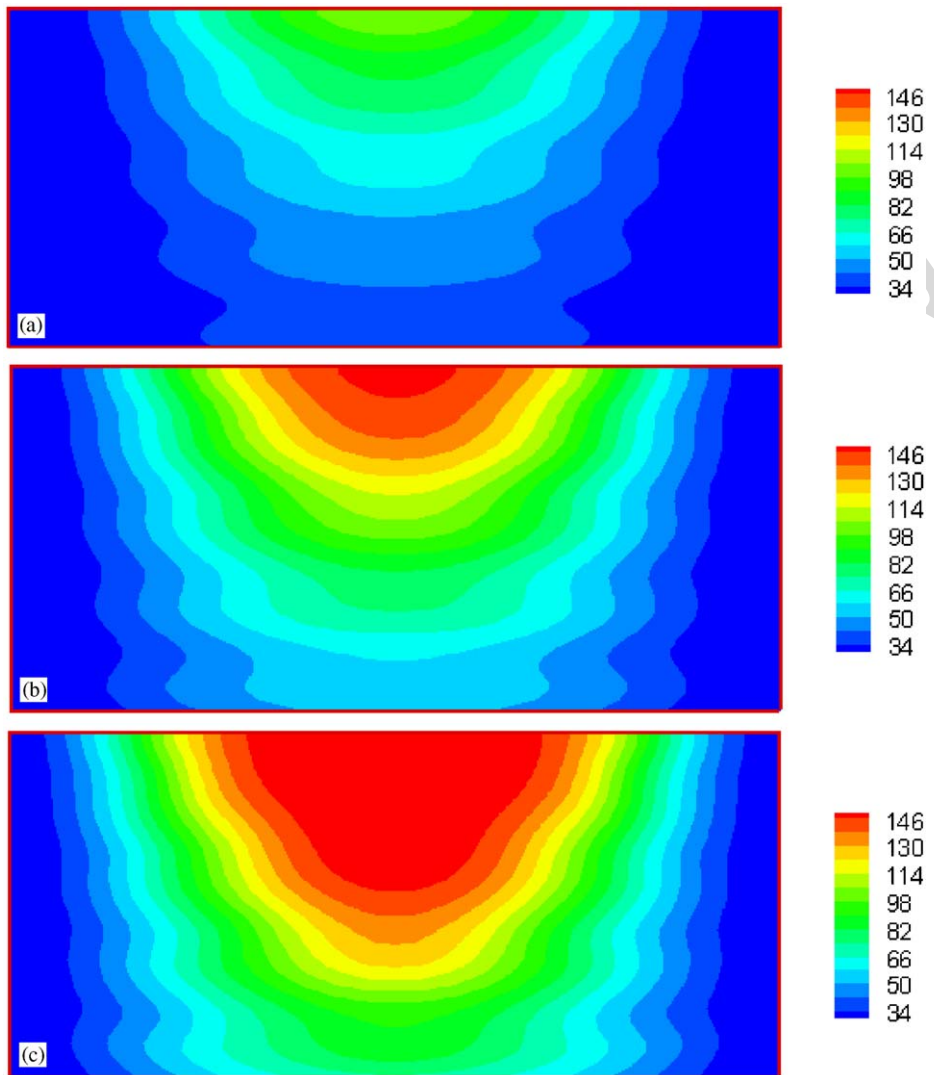


Fig. 13. Temperature distribution (°C) at various heating times: (a) 10 s; (b) 20 s; (c) 30 ($f = 2.45$ GHz, size = 11 cm (x) \times 8 cm (z)).

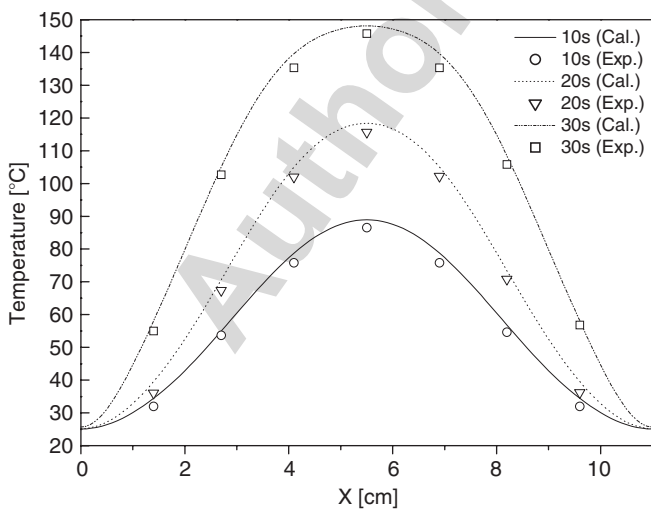


Fig. 14. Temperature distribution in wood sample along horizontal axis ($z = 0.5$ cm) ($f = 2.45$ GHz, size = 11 cm (x) \times 5 cm (z)).

distribution as well as temperature distribution within the sample display a wavy behavior due to the thickness of sample is close to the penetration depth. This causes a resultant of a transmitted wave at the incident face and a reflected wave from the end surface. Most of heating occurs at the center of the test sample where the electric field is maximum for this standing wave configuration. The thicker sample leads to lower intensity of the reflected wave, the contribution from reflected wave is weak and the power distribution as well as temperature distribution display a weak wavy behavior similar to that an attenuated transmitted wave. For the higher frequency (frequency of 5 GHz) the power absorbed at the surface increases and the decay in to the sample is more rapid. In this case, the contribution from reflected wave is negligible and power distribution behaves similar to that an attenuated transmitted wave, as in the case of the Lambert law solution.

The presented modeling is used to identify the fundamental parameters, and provides guidance for the study of microwave drying of wood in the future.

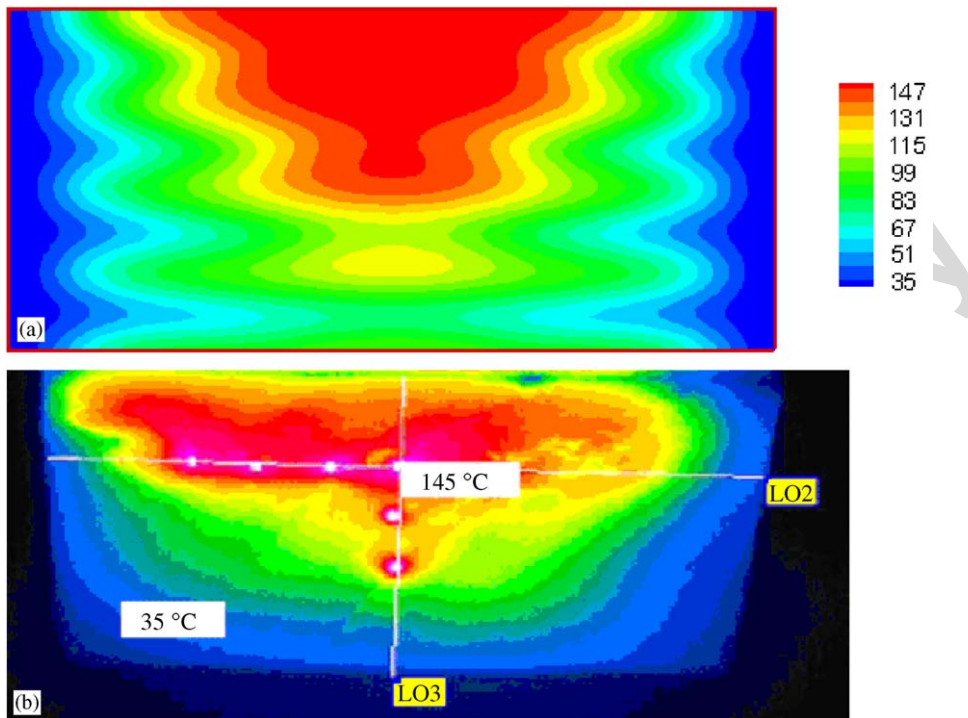


Fig. 15. The comparison of temperature distribution (°C) in wood sample: (a) simulated result; (b) experimental result ($f=2.45$ GHz, size=11 cm (x) \times 5 cm (z)).

	$f = 2.45$ GHz size = 11 cm (x) \times 5 cm (z)	$f = 5$ GHz size = 11 cm (x) \times 5 cm (z)	$f = 2.45$ GHz size = 11 cm (x) \times 8 cm (z)
Temperature Distribution			
Microwave Power Absorbed			
Conclusions	Most of heating occurs at the center of the test sample. Heating pattern is influenced by resonance. The strong wavy behavior within the sample is formed.	Most of heating occurs at the center of the test sample. Heating pattern is not influenced by resonance. The wavy behavior within the sample is totally absent.	Most of heating occurs at the center of the test sample. Heating pattern is influenced by resonance. A weak wavy behavior within the sample is formed.

Notation

B	magnetic flux density, Wb/m ²	P	power, W
C_p	specific heat capacity, J/kgK	Q	local electromagnetic heat generation term, W/m ³
D	electric flux density, C/m ²	T	temperature, C
E	electric field intensity, V/m	t	time, s
f	frequency of incident wave, Hz	$\tan \delta$	loss tangent, dimensionless
H	magnetic field intensity, A/m	Z_H	wave impedance, Ω
		Z_I	intrinsic impedance, Ω

Greek letters

ε	permittivity, F/m
λ	wavelength, m
μ	magnetic permeability, H/m
v	velocity of propagation, m/s
ρ	density, kg/m ³
σ	electric conductivity, S/m
ω	angular frequency, rad/s

Subscripts

g	wave guide
n	component of normal direction
r	relative
t	component of tangent direction
x, y, z	coordinates
0	free space, initial condition

Acknowledgments

The author is pleased to acknowledge Thailand Research Fund (TRF) and National Metal and Materials Technology Center (MTEC) for supporting this research work. Prof. K. Aoki of the Nagaoka University of Technology has valuable recommendation in this research area the author is also grateful.

References

- Ayappa, K.G., Davis, H.T., Crapiste, G., Davis, E.A., Gordon, J., 1991. Microwave heating: an evaluation of power. *Chemical Engineering Science Journal* 46, 1005–1016.
- Ayappa, K.G., Davis, H.T., Davis, E.A., Gordon, J., 1992. Two-dimensional finite element analysis of microwave heating. *A.I.Ch.E. Journal* 38, 1577–1592.
- Basak, T., 2003. Analysis of resonances during microwave thawing of slabs. *International Journal of Heat and Mass Transfer* 46, 4279–4301.
- Basak, T., 2004. Role of resonances on microwave heating of oil-water emulsions. *A.I.Ch.E. Journal* 50, 2659–2675.
- Metaxas, A.C., Meredith, R.J., 1983. *Industrial Microwave Heating*. Peter Peregrinus Ltd., London.
- Mujumdar, A.S. (Ed.), 1995. *Handbook of Industrial Drying*. second ed., Marcel Dekker, New York.
- Perre, P., Turner, W., 1997. Microwave drying of softwood in an oversized waveguide. *A.I.Ch.E. Journal* 43, 2579–2595.
- Rattanadecho, P., 2004. The theoretical and experimental investigation of microwave thawing of frozen layer using microwave oven (Effects of layered configurations and layered thickness). *International Journal of Heat and Mass Transfer* 47, 937–945.
- Rattanadecho, P., Aoki, K., Akahori, M., 2001. A numerical and experimental study of microwave drying using a rectangular wave guide. *Drying Technology International Journal* 19, 2209–2234.
- Rattanadecho, P., Aoki, K., Akahori, M., 2002. Influence of irradiation time, particle sizes and initial moisture content during microwave drying of multi-layered capillary porous materials. *ASME Journal of Heat Transfer* 124, 151–161.
- Saltiel, C., Datta, A., 1997. Heat and mass transfer in microwave processing. *Advances in Heat Transfer* 30, 1–94.
- Tada, S., Echigo, R., Kuno, Y., Yoshida, H., 1998. Numerical analysis of electromagnetic wave in partially loaded microwave applicator. *International Journal of Heat and Mass Transfer* 41, 709–718.
- Zhao, H., Turner, I.W., 2000. The use of a coupled computational model for studying the microwave heating of wood. *Applied Mathematical Modeling* 24, 183–197.